SCATTER OF FRACTURE TOUGHNESS IN THE DUCTILE-BRITTLE TRANSITION REGION

W.Ehl[1], D.Munz[1], A.Brückner[2]

In the ductile-brittle transition region of ferritic steels an effect of specimen size on the fracture toughness parameters and large amount of scatter is observed. A weakest link model including the effect of stable crack extension is presented and compared with experimental results of the reactor steel 20 MnMoNi 55. This model was not able to explain the size effect. Therefore is was tentatively concluded that in addition to the statistical effects the fracture is influenced by the stress state, which is dependent of the thickness and is changing during crack extension.

INTRODUCTION

Fracture mechanics tests conducted at various temperatures with specimens of ferritic steels yield the following features (Keller and Munz (1)):

- brittle, cleavage fracture at low temperatures,
- cleavage fracture after some amount of ductile tearing at intermediate temperatures
- ductile tearing beyond maximum load at higher temperatures

Two additional effects are observed especially in the intermediate temperature range:

- large amount of scatter of the critical value of the J-integral at the onset of cleavage fracture, whereas much less scatter is observed for the ductile J-Δa-curve (Fig.1);

1) University of Karlsruhe, FR Germany
2) Nuclear Research Center, Karlsruhe, FR Germany

- large effect of specimen size, especially specimen thickness, on the onset of cleavage fracture (increasing toughness with decreasing thickness).

Both effects have been explained by a weakest link model based on the assumption that failure starts from a weak point near the crack front where the weak points are statistically distributed in the material. The thickness effect then is caused by the higher probability of having a weak point near the crack front for a thicker specimen. This model was used first by Landes and Shaffer (2). In the form presented it should apply only to cleavage crack extension not preceded by ductile tearing. Some of the specimens of Landes and Shaffer showed, however, some stable crack extension. Brückner and Munz (3) extended the weakest link model to include the effect of stable crack extension.

The size effect can be influenced in addition by the effect of constraint (Sumpter (4), Milne and Chell (5)). In suffiently thick specimens a state of plane strain can be expected to occur along most part of the crack front. With decreasing thickness of the specimens the stress component σ_z in the direction of the crack front gets more and more important, leading to less constraint at the crack tip and, therefore, to an increase in toughness.

In this paper experimental results are compared with the prediction by the model developed by Brückner and Munz.

WEAKEST LINK MODEL INCLUDING STABLE CRACK EXTENSION

The assumption made for the model presented in reference (3) are:

1. There are two independent fracture modes, ductile tearing and cleavage. Ductile tearing can be described by a material resistance curve in terms of J_{IR} or K_{IR} as a function of the crack extension Δa, which is independent of the size of the specimens.
2. Unstable cleavage crack extension starts from weak points in the material, for instance from inclusions. Therefore, the distribution of these weak points of different sizes is responsible for the scatter in the onset of cleavage cracking. This can be described by the local distribution of the toughness of the material. Where linear-elastic fracture mechanics can be applied, the toughness parameter

is K_{Icl} (cl = cleavage). If cleavage cracking starts after a large amount of plastic deformation, the toughness parameter should be the critical value of the J-integral J_{Icl}. It can, however, be argued whether the J-integral or the elastic energy release rate is triggering the onset of cleavage crack extension (Turner (6)).

3. It is assumed that there is no change in constraint during stable crack extension.
4. A constant value of K or J along the crack front is assumed.

The model is presented first in terms of the stress-intensity factor. Small units of area in front of the crack tip of length λ and width ω are considered. Each of these areas is attributed a specific value of K_{Icl}. The scatter of K_{Icl} is described by a Weibull distribution with cumulative density function

$$F\langle K_{IC}\rangle = 1 - \exp\left[-\left(\frac{K_{IC}}{b_\lambda}\right)^{m_\lambda}\right] \tag{1}$$

For a crack of front length L the probability that no cleavage fracture occurs is a function of the applied stress intensity factor K_{Iappl} and the ration L/λ:

$$P_S = \left[1 - F\langle K_{Iappl}\rangle\right]^{L/\lambda} = \exp\left[-\left(\frac{K_{Iappl}}{b_\lambda}\right)^{m_\lambda}\frac{L}{\lambda}\right] \tag{2}$$

At the onset of stable crack extension for $K_{Iappl} = K_{Ii}$ the following relation applies:

$$P_S = \exp\left[-\frac{K_{Ii}}{b_\lambda}^{m_\lambda}\frac{L}{\lambda}\right] = \exp\left[-\frac{K_{Ii}}{b_L}^{m}\right] \tag{3}$$

with

$$m = m_\lambda \tag{4}$$

$$b_L = b_\lambda \cdot \left(\frac{\lambda}{L}\right)^{1/m} \tag{5}$$

$P_f = 1 - P_S$ is the probability of cleavage cracking before the onset of stable crack extension. If the crack extends stably by Δa, there will be $\Delta a/\omega$ additional samples of L/λ unit areas. For the special case that during crack extension $K_{IR} = K_{Ii} = \text{const.}$ (flat crack growth resistance curve), the survival

probability is

$$P_S = P \text{ (survival at the onset of stable crack extension)} \times P \text{ (survival after stable crack extension)}$$

$$= \left[1 - F\langle K_{Ii}\rangle\right]^{L/\lambda} \left\{\left[1 - F\langle K_{Ii}\rangle\right]^{L/\lambda}\right\}^{\Delta a/\omega}$$

$$= \exp\left\{-\left(\frac{K_{Ii}}{b_\lambda}\right)^{m_\lambda} \frac{L}{\lambda}\left(1 + \frac{\Delta a}{\omega}\right)\right\} \qquad (6)$$

For a rising crack-growth resistance curve, Eq. (6) has to be replaced by (see reference (3))

$$P_S = \exp\left\{-\left(\frac{K_{Ii}}{b_\lambda}\right)^{m_\lambda} \frac{L}{\lambda}\left[1 + \frac{1}{\omega}\int_0^{\Delta a}\left(\frac{K_{IR}}{K_{Ii}}\right)^{m_\lambda} d(\Delta a)\right]\right\} \qquad (7)$$

The failure probability then is

$$P_f = 1 - P_S = 1 - \exp\left\{-A_L\left[1 + \frac{1}{\omega}\int_0^{\Delta a}\left(\frac{K_{IR}}{K_{Ii}}\right)^{m} d(\Delta a)\right]\right\} \qquad (8)$$

with

$$A_L = \left(\frac{K_{Ii}}{b_L}\right)^m \qquad (9)$$

$$b_L = b_\lambda\left(\frac{\lambda}{L}\right)^{1/m} \qquad (10)$$

$$m = m_\lambda \qquad (11)$$

Equation (8) can also be interpreted as the cumulative density function of the stable crack extension until cleavage cracking.

Instead of the stress intensity factor K_I the J-integral can be used. Then K_I has simply to be replaced by J_I in Eq. (8):

$$P_f = 1 - \exp\left\{-A_L\left[1 + \frac{1}{\omega}\int_0^{\Delta a}\left(\frac{J_{IR}}{J_{Ii}}\right)^{m} d(\Delta a)\right]\right\} \qquad (12)$$

with

$$A_L = \left(\frac{J_{Ii}}{b_L}\right)^m \qquad (13)$$

In Fig. 3 the distributions expected from this model are shown schematically. For a flat crack-growth resistance curve the maximum possible stress intensity factor is K_{Ii} at the onset of ductile tearing. For a rising crack-growth resistance curve a deviation from the linear Weibull-plot occurs for $K_I > K_{Ii}$. If the load displacement curve has a small slope, an upward trend in the Weibull-plot is expected. For an J-integral evaluation, in which the area under the load-displacement curve is important, a different shape of the curve is expected.

EXPERIMENTAL PROCEDURE

Compact tension specimens with a width W = 50 mm of the 20 MnMoNi 55 reactor steel (similar to A 533 B) were tested. The thickness was B = 25 mm, B = 12,5 mm and B = 5mm. All specimens with B = 25 mm and B = 12,5 mm had side grooves (reduced thickness $B^* = 21$ mm; 9,5 mm). Some of the 5 mm thick specimens had side grooves ($B^* = 4$mm), the others were tested without side grooves. The relative crack length after precracking in fatigue was about a/W = 0,6. The tests were performed at -40°C. All specimens with B = 25 mm and B = 21,5 mm were loaded until the onset of brittle fracture. Some of the specimens with B = 5 mm were unloaded before brittle failure occurred in order to obtain J-values for different stable crack extension.

The J-integral was calculated from the area under load-load point displacement curve U:

$$J = \frac{2\ D\ U}{B\ (W-a)} \tag{14}$$

with

$$D = \frac{1 + \gamma}{1 + \gamma^2}\ , \qquad \gamma = \frac{\sqrt{2\left[1 + (a/W)^2\right]} - (1 + a/W)}{1 - a/W} \tag{15}$$

The stable crack extension was measured at nine points excluding the stretched zone. For small crack extensions the area of ductile tearing was measured and devided by the thickness B^* .

EXPERIMENTAL RESULTS

Origin of cleavage

The specimens have been investigated by SEM in order to find the trigger point from which the cleavage fracture starts. At low magnification one can see tear ridges, which are used to determine the general location of cleavage initiation. At higher magnification cleavage facets with river pattern can be observed and the origin of cleavage can be located.

In nearly all cases it was possible to find an origin of cleavage at the brittle fracture surface. In most cases one large facet or a group of adjacent facets constitutes the origin of cleavage. In 20% of all specimens a particle or a small hole has been detected within the facets as the point of initiation. In nearly the same number of cases there is a twin or a microcrack perpendicular to the main crack plane. It seems that in these cases grains or a group of grains, which have a suitable orientation with respect to the cleavage crack, are triggering the cleavage fracture.

By SEM the distances have been measured of the origins of cleavage to the stretched zone or to the stable crack front, denoted by x, and along the crack front (distance z from the center) (Fig. 4). The results are presented in Fig. 5. One can see that most of the trigger points are not situated directly ahead of the crack front but at a distance of up to 1.5 mm. It can be seen also that the trigger points are distributed nearly uniformly over the specimen thickness, except for a 1-2 mm zone near the side grooves, in which no trigger points have been found.

J-INTEGRAL EVALUATION

Figure 6 shows the J-Δa-plot for all specimens with a stable crack extension of $\Delta a > 100$ µm. All data points correspond to different specimens and mark the onset of unstable cleavage crack extension. Only some of the 5 mm thick specimens were unloaded before the onset of cleavage.

It can be seen that the ductile J-Δa-curve is independent of the thickness of the specimens in the range where data points for all three specimen sizes were available. The J_{IR}-Δa-curve can be described by

$$J_{IR} = 670 \cdot (\Delta a)^{0.51} + 23.2 \qquad (16)$$

if Δa in mm and J_{IR} in N/mm.

The onset of ductile crack extension can be defined conveniently for a crack extension of $\Delta a = 10\mu m$. Note that the ductile crack extension is measured excluding the stretched zone. Then from Eq.(16)

$$J_{Ii} = 87.2 \text{ N/mm}$$

is obtained.

In Fig. 7 $\ln\ln 1/(1 - P_i)$ is plotted versus $\ln J_{Icl}$. The failure probability P_i is obtained by

$$P_i = \frac{i - 0.3}{n + 0.4}$$

where n is the total number of specimens and i the rank order of the individual specimens. Specimens with no stable crack extensions (less than 10 µm) are marked as solid points. For the specimens with $B^* = 4$ mm only the three values with the lowest J_{Icl} are plotted. Because of the unloading of some specimens before cleavage fracture the other specimens could not be ranked correctly.

To evaluate the test result a straight line was first fitted through the data points for those specimens with $B^* = 21$ mm, in which no stable crack extension occurred before cleavage. The Weibull parameter for these specimens are

$$m = 4.24, \quad b_{21} = 90.5$$

This Weibull distribution describes the data up to $P_f = 0.57$ (the failure probability for the onset of stable crack extension at $J_{Ii} = 87.2$ mm).

Equation (12) now can be used to predict the failure probability for the region of stable crack extension. The quantity ω - the sampling width for cleavage cracking - is unknown. It should be on the order of the distance x of the origin of cleavage from the crack front. Figure 7 includes the predictions for the average distance $\omega = 0.39$ mm and for an upper limit of $\omega = 1$ mm.

The prediction for the specimens with $B^* = 9.5$ mm and $B^* = 4$ mm are also included in Fig. 7 . For low failure probabilities within the linear part cleavage crack should start without prior stable crack extension. The Weibull parameter m is the same as for the specimens with $B^* = 21$ mm. The parameter b and the critical failure probabilities P_f are

$b_{9.5} = 109.1$, $P_f = 0.32$ for $B^* = 9.5$ mm

$b_4 = 133.8$, $P_f = 0.15$ for $B^* = 4$ mm

Figure 7 shows clearly that the predictions are not in agreement with the experimental results, both for failure before the onset of ductile tearing and failure after ductile crack extension. For instance, regarding the specimens with $B^* = 9.5$ mm one out of 21 tested specimens failed without stable crack extension whereas 7 failures had been predicted by the weakest link model

Within the region of stable crack-growth larger J_{Icl}-values were measured for a given failure probability than had been predicted. It was not possible to achieve better agreement by adjusting ω within a reasonable range.

CONCLUSION

The investigation on the size effect is not complete. Specimens with B = 50 mm have to be tested. The results obtained so far can be summarized:

1. Cleavage crack starts with or without prior stable crack extension at a distance up to 1.5 mm ahead of the crack tip.

2. Within the investigated range of the size of specimen and of the crack extension the ductile stable crack-growth can be described by one J_{IR}-Δa-curve.

3. It is not possible to predict the scatter of the J-integral at the onset of cleavage cracking of the specimens after stable crack extension applying a weakest link model with the assumption of no change of the stress state at the tip of the crack.

The initiation of cleavage cracking ahead of the crack tip was also observed by Rosenfield and Shetty (7). It is related to the stress distribution near

the crack tip which has a broad maximum. Cleavage fracture is initiated if the stress reaches a critical value at a weak point ahead of the crack tip. A detailed model is given by Wallin et al (8). Therefore cleavage cracking without prior stable crack extension should start somewhere within the maximum stress range. For cleavage cracking after ductile tearing a weak point reaches its critical cleavage stress always ahead of the advancing crack. A more detailed evaluation of the distance x is given elsewhere (Ehl, Munz, Brückner (9)).

The size effect can be tentatively explained by an effect of thickness and of ductile crack extension on the constraint ahead of the crack tip. Applying the requirements for plane strain J_{IC}- evaluation

$$B,\ W-a > 25\ \frac{J_{IC}}{\sigma_y}$$

as an indication with σ_y = 497 MPa, valid J_I-values should be obtained up to J_I = 496 N/mm for ^{I}B = 25 mm, J_I = 249 N/mm for B = 12,5 mm, J_I = 99 N/mm for B = 5 mm. As expected the ductile J_{IR}-Δa-curve is independent of the size of the specimens within this range. With regard to cleavage cracking obviously the size requirement has to be modified. Without an exact knowledge of the three-dimensional stress distribution ahead of an advancing crack no detailed explanation can be made. It seems, however, that cleavage cracking is much more susceptible to the stress state at the crack tip and that this stress state changes during stable ductile crack extension.

REFERENCES

(1) Keller, H.P., and Munz, D., Fracture and Fatigue, ECF3, Pergamon Press, 1980, pp. 105 - 117

(2) Landes, J.D., and Shaffer, D.H., ASTM STP 700, 1980, pp. 368 - 382, Fracture Mechanics: Proceedings of the Twelvth National Symposium on Fracture Mechanics

(3) Brückner, A., and Munz, D., Advances in Probabilistic Fracture Mechanics - PVP - Vol. 92, The American Society of Mechanical Engineers, 1984, pp. 105 - 111

(4) Sumpter, J.D.G., Metal Science, Vol. 10, 1976, pp. 354 - 356

(5) Milne, I., and Chell, G.G., Elastic-Plastic Fracture Mechanics, ASTM STP 668, 1979, pp. 358 - 377

(6) Turner, C.T., Post-Yield Fracture Mechanics, Second Edition, Elsevier Applied Science Publishers, 1984, pp. 25 - 221

(7) Rosenfield, A.R., and Shetty, D.K., Elastic-Plastic Fracture Test Methods: The User's Experience, ASTM STP 856, 1985, pp. 196 - 209

(8) Wallin, K., Saario, K., and Törrönen, K., Metal Science, Vol. 18, 1984, pp. 13 - 16

(9) Ehl, W., Munz, D., and Brückner, A., Seminaire International sur L'Approche Locale de la Rupture, Fontainebleau, 1986.

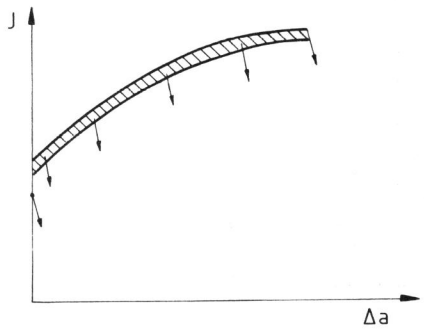

Fig.1: Scatter of the onset of cleavage cracking

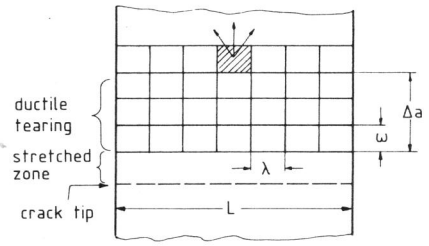

Fig.2: Cleavage after ductile tearing

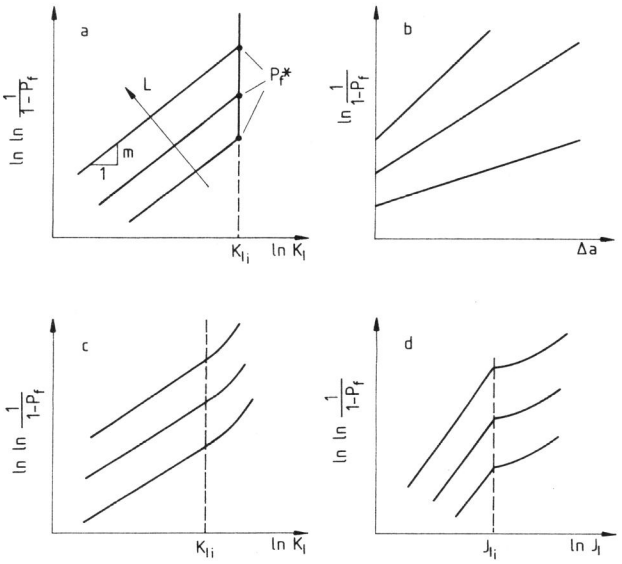

Fig.3: Expected distributions for cleavage after stable crack extension

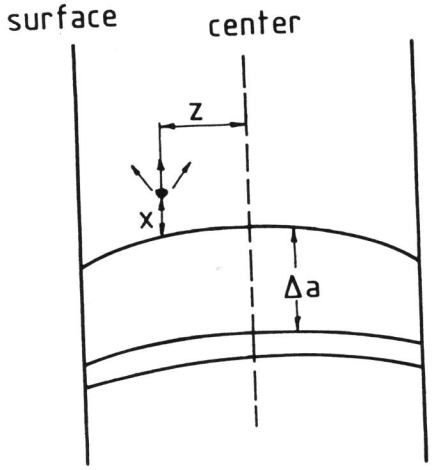

Fig.4: Location parameter x and z for onset of cleavage cracking

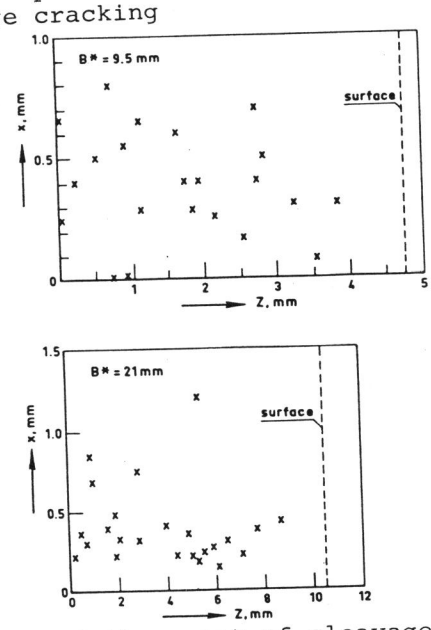

Fig.5: Location of the onset of cleavage cracking

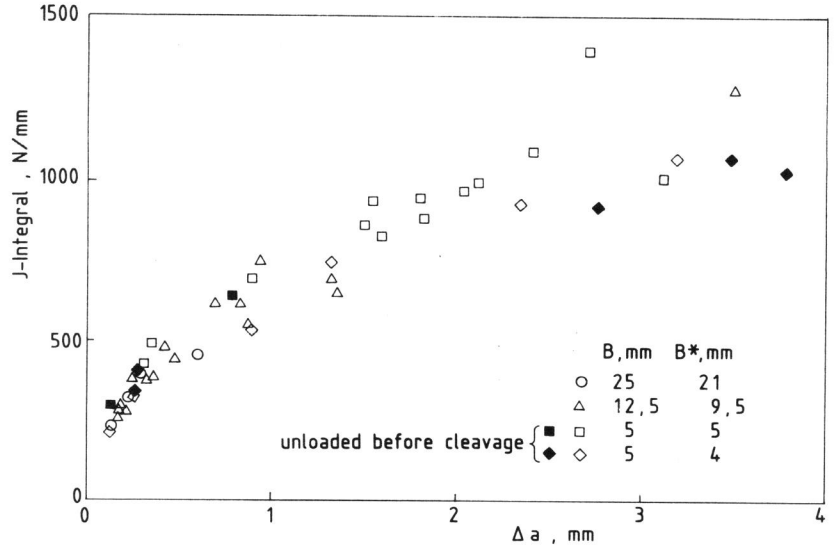

Fig.6: J_I-Δa-curve

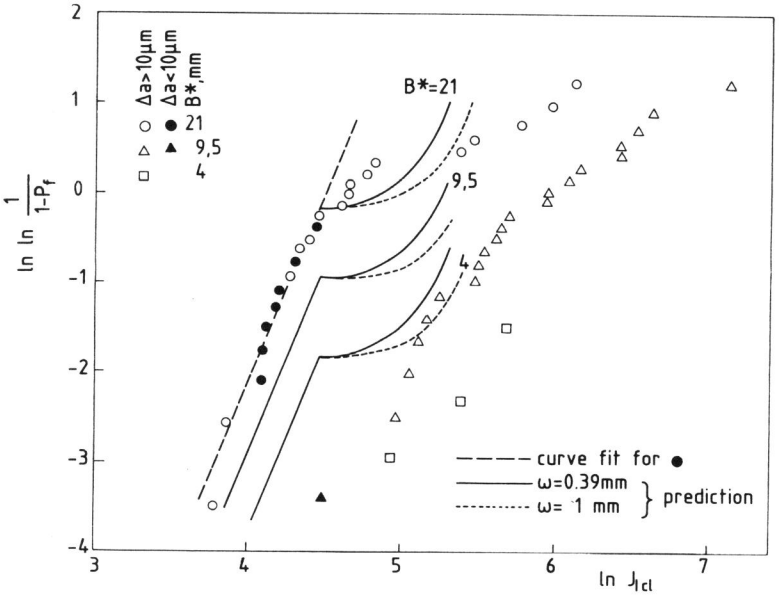

Fig.7: Failure probability for cleavage cracking